SCHOOL OF PHYSICS AND ASTRONOMY

YEAR 4 PROJECT DISSERTATION

SESSION 2017-2018

Name:	**Amanda Seedhouse**
Student Number:	**1476337**
Degree Programme:	**MPhys Physics**
Project Title:	**What can a muon tell us about the behaviour of magnetic systems?**
Supervisor:	**Dr S Giblin**
Primary Assessor:	**Dr D I Westwood**
Second Assessor:	**Professor J E Macdonald**

Declaration:

I have read and understand Appendix 2 in the Student Handbook: "Some advice on the avoidance of plagiarism".

I hereby declare that the attached report is exclusively my own work, that no part of the work has previously been submitted for assessment (although it may re-use material from the "Summary Report" for **this project** as it is considered part of the same assessment), and that I have not knowingly allowed it to be copied by another person.

What can a muon tell us about the behaviour of magnetic systems?

Amanda Seedhouse

Abstract

A model of the muon spin relaxation (μSR) experiment was constructed to be able to understand the implantation distribution of muons. This is necessary since the muon implantation sites contribute to a large error in experiments. Muons in close proximity to a magnetic sample are thought to feel the magnetic dipole contributions from the sample more uniformly in comparison to being inside the sample. The code simulates the μSR experiment to find any non-uniformity of magnetic field measurement. The computational simulation involves adjusting the implantation depth and beam spot size of the muons to see how the magnetic field and relaxation rate of the systems change. It was found that both of these factors were affected by the muon distribution changing and can be compared to μSR results to determine any unexpected deviations from the experimental outcomes.

Contents

1 Introduction

The muon, a spin 1/2 unstable elementary particle discovered in 1936 by Carl Anderson and Seth Neddermeyer [1], has proven to be a useful probe when examining properties of materials on the atomic scale. A beam of spin polarised muons is particularly applicable when it comes to measuring small magnetic fields of matter. The muons can be inserted into a stopping material, see section 1.1 for details. There, they thermalise and are perturbed by an applied magnetic field causing muon spin precession. It is this precession that enables the measurement of magnetic fields via muon spin relaxation (μSR) experiments. Section 2.1 gives specifics of the μSR experiment.

Within the stopping material the thermalised muons stop at different sites forming a distribution. How the distribution of muons can affect the measurements made in the μSR experiment is not completely understood. This report aims to shed light in this area by means of a computational model. The model is used to demonstrate what happens to the measurement of local magnetic fields depending on the distribution of muons, building up from a single magnetic nanoisland with a single muon to a system with multiples of both.

Small magnets such as nanoislands and single molecule magnets have the potential to improve information storage density [2]. Through the use of such magnets it may be possible to store information at the molecular level, with each magnet serving as a storage unit [3] with information encoded in the spin of atoms. A greater understanding of the properties of these small magnets will be advantageous for the science of magnetic materials and their applications.

μSR has many advantages over other local probe techniques, such as nuclear magnetic resonance (NMR) or Mössbaur spectroscopy, include the fact that a muon can; be implanted into many materials, has low enough energy to stop within a suitable thickness of a material, and a beam of polarised muons is obtainable through the decay of pions.

1.1 Muon implantation

This report will be focussing on low energy μSR [4] where muons are implanted into a stopping material that does not change the polarisation of the incoming muons [5]. The idea behind this method is to ensure that the muons are not modifying the field distribution of the sample being measured. This in turn would produce more reliable results. The magnetic field of a material felt by a muon is approximately the summation of individual magnetic dipoles of the system [6]. The problem with muons being implanted into the material being measured is that the contribution of each magnetic dipole will not be uniform. Measuring the magnetic field in close proximity to the material tries to overcome this. For muons situated outside of the material the contribution of individual dipoles felt will be more uniform. This aims to create a more predictable probe. The objective of this report is to simulate the muon distribution in the μSR experiment to see if they return unbiased predictions of the measured magnetic field distributions of magnetic materials.

In μSR experiments the position of each muon will differ with the stopping material. There have been investigations into the muon stopping sites within materials [7]. It is important that the distribution of muons inside this stopping material is known in order to interpret μSR results properly. It is shown that the largest source of systematic error in μSR experiments is the muon implantation profile [8]. The profile is often calculated using an ion implantation code for example TRIM.SP [9]. Simulations like TRIM.SP treat the muon as a light proton which has a mass $1/9^{th}$ that of the proton. Using a Monte-Carlo technique the simulation predicts the path of a particle inside a solid including the collision processes that occur inside a structure.

If the muons are being stopped outside of a magnetic sample then experiments should be performed on thin films. Examples of this include the study of a flux distribution across a $YBa_2Cu_3O_{7-\delta}$ surface [10] and superparamagnetism in Fe nanoclusters [11]. Stopping materials are chosen such that they do not cause considerable precession of the implanted muons [12, 13]. This is necessary since the only relaxation rate that should be measured is that from the magnetic film.

The implantation profile is dependent on the stopping material, the energy of the incoming muon, and can also be adjusted by applying an external magnetic field [14]. This means that when modelling the muon distribution various widths and depths of the muons can be examined. In μSR experiments the implantation energy and therefore depth distribution are small, for example from 5nm to 200nm [15]. The size of the stopping material will determine the average implantation depth of the muons and the size of the incoming muon beam will determine the spread of muons in the other two coordinates.

2 Theory

2.1 Muon spin relaxation

Relevant details of the μSR experiment and the theory behind muon relaxation will be covered in the section, taking any derivations from [16]. This aims not to give a full picture behind the μSR experiment, but to provide the essential knowledge that will be used in the computational model and will enable the reader to understand the discussion points of the report.

μSR is a method of measuring the local magnetic environment of a material utilising the parity violation found in the decay of the muon. Perfectly spin-polarised muons created in the decay of a pion [16] will change their polarisation depending on the surrounding environment. This was realised while searching for appropriate stopping materials for positive muons (μ^+) [17]. In the presence of a magnetic field the spin vectors of the produced muons change. If the field is off-axis with respect to the spin of the muon then the precession is at the Larmor frequency ω, related to the magnetic field as follows:

$$\omega = \gamma_\mu \mathbf{B}. \tag{1}$$

The magnetic field in Tesla is $\mathbf{B}$ and $\gamma_\mu = 2\pi \times 135.5\text{MHzT}^{-1}$, the gyromagnetic ratio for a muon [18].

To obtain a measurement of the direction of the muon spin polarisation μSR uses the decay of positive muons into positrons. The decay of a positive muon into a positron, electron neutrino and muon anti-neutrino is shown:

$$\mu^+ \rightarrow e^+ + \nu_e + \bar{\nu_\mu}.$$

Here the use of positively charged muons is essential because their lifetime in most materials is $2.2\mu s$, whereas the lifetime of negatively charged muons is dependent on the atomic number of the material they are embedded in [19]. The mass of a muon is greater than that of an electron, thus a negative muon may displace an electron from a nearby atom because it is attracted to the nuclei, unlike a positive muon.

The positron is emitted in a direction governed by the probability distribution

$$W(\theta) = 1 + a\cos(\theta) \tag{3}$$

with θ being the angle between the spin of the muon and the direction of the positron and a is the asymmetry factor. The maximum value of W occurs when θ is a multiple of $2n\pi$, $n = 0, 1, 2, ...$, which means that the e^+ emits preferentially in the direction of the muon's spin. Exploiting this fact, μSR experiments use the detection of the emitted positrons to determine the polarisation direction of the muon. The muons are stopped either within or in close proximity to the material of interest. As the muon thermalises there is no significant loss from its initial polarisation. Following this, the emitted positrons are counted in two detectors that are located at opposing positions with respect to the muon distribution, see figure 1. Thus the muon spins can be determined as a function of time. To determine this an asymmetry value, α_0, can be found from the difference in number of positrons observed in the backward (N_B) and forward (N_F) facing detectors,

$$\alpha_0(t) = \frac{N_B(t) - N_F(t)}{N_B(t) + N_F(t)}. \tag{4}$$

In a transverse magnetic field the asymmetry for a single muon should resemble a cosine wave. This is because at time = 0, $\alpha_0 = 1$, i.e. the spin vector has had no time to precess. This means it will be counted in N_B. As time progresses, α_0 also shifts eventually coming to $\alpha_0 = -1$. Obviously a single muon can not be emitting positrons at all times, it will decay once. This is why in experiments numerous muons are used.

As the angle θ of the magnetic field with respect to the spin changes, the asymmetry will also change. This is because the spin has multiple components. In the transverse field where $\theta = \pi/2$ rad there is a single precession, in a longitudinal field $\theta = 0$ rad there is no precession. The precession between angles can be described using

$$\sigma(\theta, t) = \cos^2(\theta) + \sin^2(\theta)\cos(\gamma_\mu \mid \mathbf{B} \mid t) \tag{5}$$

for time t, where σ is the spin polarisation. Going back to the example of a single muon in a transverse field it can be seen that $\sigma = \cos(\gamma_\mu \mid \mathbf{B} \mid t)$, an asymmetry resembling a cosine wave.

In some materials the local fields are randomly orientated. Since the muon distribution is three dimensional it can be approximated that $1/3$ of the local fields are aligned with the muon spin, so $\cos^2(\theta) = 1/3$. The other $2/3$ will allow the muon to precess leading to equation 5 becoming the relaxation function

$$G(t) = \frac{1}{3} + \frac{2}{3}\cos(\gamma_\mu \mid \mathbf{B} \mid t). \tag{6}$$

Where the muon thermalises in the stopping material it will feel the magnetic field from the nuclei of the sample that is being measured. A vector sum of the fields from the nuclei can be approximated as a Gaussian so that the zero-field relaxation function can be found by averaging equation 6 over a Gaussian distribution.

$$G(t) = \frac{1}{3} + \frac{2}{3}(1 - \Delta^2 t^2)e^{-\Delta^2 t^2/2} \tag{7}$$

where Δ is the width of random fields. This is known as the Kubo-Toyabe function [20], it has a persisting $1/3$ asymmetry and $2/3$ component showing a damped oscillation at $\gamma_\mu \mid \mathbf{B} \mid$. This function is plotted in figure 2 and can only be seen in a system with multiple muons. The plot can be thought of as the sum of the individual relaxation functions G of the different muons positioned at various sites near the

magnetic material. Each muon will feel a different magnetic field due to its position with respect to the magnetic sample. This leads to various relaxation functions, each with their own phase. As the relaxation functions of each muon are summed along with the respective phases, its result should follow the Kubo-Toyabe distribution. Since it would be unreasonable to model the experiment based on forward and backward detectors, the summation as presently described will be the basis of the computational model due to computational difficulty.

The polarisation of the muon can be shown to follow the damping signal:

$$P = P_0 e^{\lambda t} cos(\omega t) \tag{8}$$

where λ is the relaxation rate of the oscillations, ω is the precession frequency in equation 1 and P_0 is a constant describing the initial polarisation. The relaxation function and precession frequency will be the ground on which the analysis will be performed on. The relaxation function gives us information about the magnetic field distribution felt by the muons in the stopping material. A large relaxation function describes a system where the field distribution is changing a dramatically across the volume that the muons are implanted, whereas a small λ tells us that the field distribution is more uniform. The precession frequency defines the magnetic field strength as mentioned previously (equation 1).

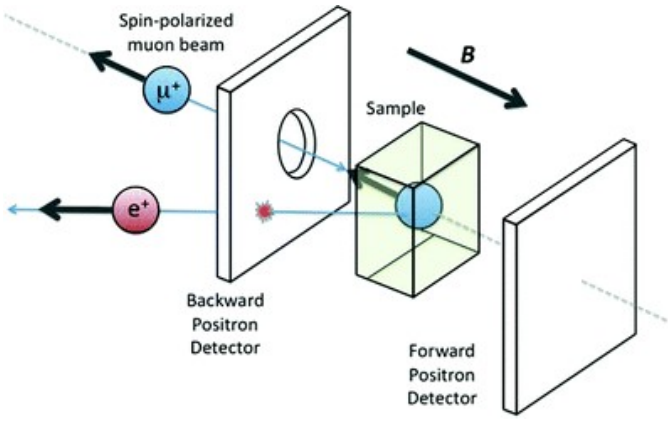

Figure 1: Schematic of the μSR experiment in a longitudinal field taken from [21]

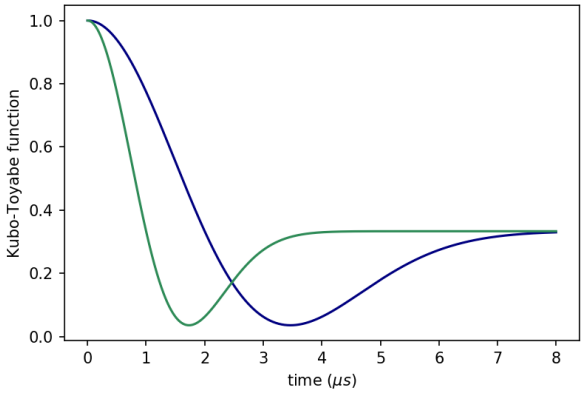

Figure 2: The Kubo-Toyabe function (equation 7) for a muon distribution in a randomly orientated magnetic field where $\Delta = 0.5\text{s}^{-2}$ (blue line) and $\Delta = 1.0\text{s}^{-2}$ (green line).

2.2 Single molecule magnets

Ferromagnets contain a number of small regions called domains where the local magnetisation reaches saturation, that magnetisation can not increase further. Each domain in a material is separated by a domain wall. As a magnetic sample reduces in size the surface energy of the sample becomes large relative to the volume energy. This is due to the fact that surface energies scale as the square of the sample size, whereas the volume energy scales as the cube of the sample size. With certain dimensions the magnetic sample will no longer have any domain walls leaving a single magnetised domain because this will be energetically favourable [18].

In the computational model single domain magnets will be of interest since nanoislands, and similar,

are small enough that they would have a single domain. Single domain magnets behave like small bar magnets which, in their simplest form, can be approximated as magnetic dipoles, following the equation [22]:

$$\mathbf{B}(\mathbf{r}) = \frac{\mu_0}{4\pi}\left(\frac{3\mathbf{r}(\mathbf{m}\cdot\mathbf{r})}{r^5} - \frac{\mathbf{m}}{r^3}\right). \tag{9}$$

B is the magnetic field in Tesla felt at a distance **r** from the magnetic dipole, μ_0 is the magnetic constant, it equals $4\pi \times 10^{-7}$H. The magnetic moment of the dipole is **m**. When dealing with multiple magnetic dipoles the field felt at a position **r** is simply the sum of each individual dipole.

3 Methodology

3.1 Single dipole magnet

The model for a magnetic nanoisland will begin with a single dipole. The magnetic field will be calculated using equation 9. The field distribution of such a magnet is shown in figure 3 using the values: **r** = (r_x, r_y, 100) μm and **m** = (0, 8.0×10^{-8}, 0) Am^2 for changing coordinates r_x and r_y. The magnetic moment will be limited to the y direction so that the field distribution is easy to compare to that of a bar magnet. When the number of dipoles is increased the model will be comparable to a thin magnetic film wherein all the magnetic moments of the nanoislands are all facing the same way. Experimentally this is done by applying a magnetisation perpendicular to the to the muon spin polarisation to cause nanoislands to become aligned, this also causes the nanoislands to become single domain magnets [12]. The field lines as seen in figure 3, represented as black arrows, are typical of a single dipole or bar magnet. The magnitude of the magnetic field is also shown as a colour map with the position of the dipole indicated by a shaded square in the centre of the figure. Again, this colour map is what one would expect from a single dipole.

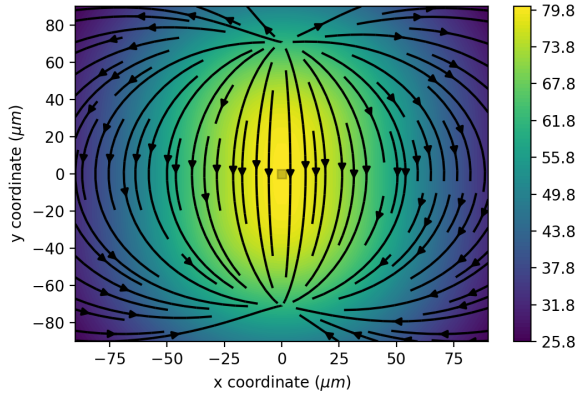

Figure 3: Magnetic field distribution for a single dipole from a r_z distance of 100μm. The shaded square in the centre shows the position of the dipole, the black lines are magnetic field lines in the x and y directions and the colour bar shows the magnitude of the magnetic field in Gauss.

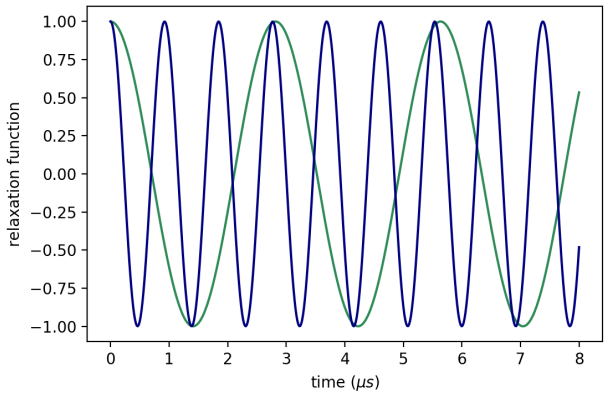

Figure 4: The relaxation function of the magnetic field felt by a single muon at the maximum magnetic field felt (from figure 3) at 80.0 G (blue line) and minimum field felt at 26.2 G (green line) for a single dipole at a z distance of 100μm.

To represent the magnetic field at a single point we utilise the relaxation function from equation 5. As described in section 2.1, the relaxation function should resemble a cosine wave because the magnetic field at a single point is not changing, therefore the precession of the muon should be uniform. Figure 4 illustrates single frequency precessions at two separate points, one where the magnetic field is at its largest (blue line) and one where it is at its smallest (green line). It is clear from the plot that the frequency is larger when the magnetic field is larger, consistent with equation 1. The 8μs time in the figure is set because in experiments this is the time window in which the relaxation can be measured [6].

3.2 Multiple magnets

A film of nanoislands is of more interest than a single nanoisland for technological applications [23]. Our model should increase the number of dipoles. Figure 5 shows a model of one hundred dipoles situated at the position of each nanoisland. The same parameters are used from section 3.1 but now at the position **r** the total magnetic field is the sum of the individual fields from each dipole. The field lines for the larger number of nanoislands are more homogeneous, the difference between the maximum and minimum magnetic fields is roughly a factor of two, whereas in figure 3 the difference between the maximum and minimum fields is a factor of approximately three. This shows us how the change of the number of dipoles can impact the system.

From equation 9 it is clear that the magnetic field should drop off with distance by a factor of $1/r^3$. To demonstrate that this is the case the magnetic field at different **r** values was calculated and normalised so that a $1/r^3$ line could be fitted to the data. This is shown in figure 6 where the dots represent the calculated magnetic field normalised and the line is a fitted $1/r^3$ function.

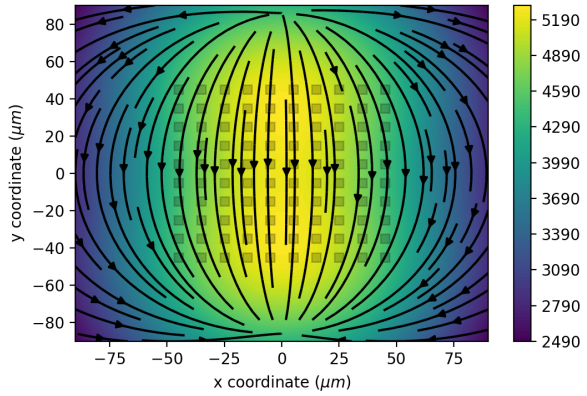

Figure 5: Magnetic field distribution for 10×10 magnetic dipoles at a r_z distance of 100μm. The translucent squares shows the position of the magnets, the lines are the magnetic field lines in the x and y directions and the colour bar gives the magnetic field in Gauss.

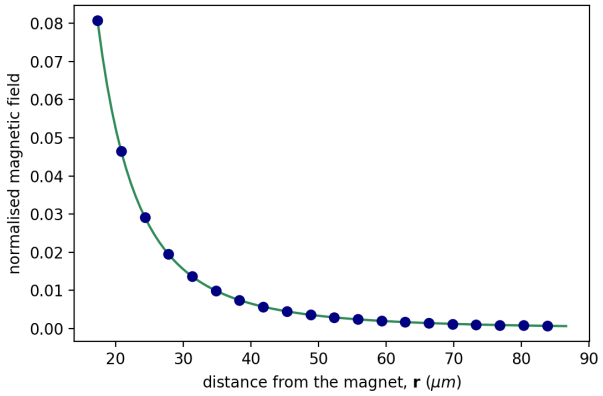

Figure 6: The magnetic field normalised at different r_z distances from the magnet source (dots) and a fitted $1/r^3$ function (line).

3.3 Gaussian muon distribution

Since the muons entering the stopping material consist of a beam it is evident that they will not spread evenly across the magnetic film. Instead, the muon beam spot follows a Gaussian distribution and should be considered in our model. To implement this, the position of the muons should be chosen randomly,

with the majority of the muons lying in the centre of the beam. If the x and y coordinates were chosen from two independent normal distributions the overall spread of the muons would not be as required. Instead the muons would gather at the means of the x and y distributions leading to a spread of muons in a plus sign shape. To overcome this the distribution can be thought of in polar coordinates where the radius, R, of the beam squared will have a normal distribution. To be able to achieve this distribution two uniform random numbers, u and v, can be chosen in the interval [0, 1] which then contribute to the radius as follows: $R^2 = u^2 + v^2$. Then, using the Box-Muller transform [24], two random coordinates, x and y, can be found from the following equations:

$$x = \sqrt{-2\ln(u)}\cos(2\pi v) \tag{10}$$

$$y = \sqrt{-2\ln(u)}\sin(2\pi v). \tag{11}$$

Figure 7 shows the distribution of muons in the x and y plane with respect to the nanoislands, the standard deviation and mean of the Gaussian distribution can be changed for the muon sites. In the figure the mean is zero and the standard deviation is 10μm in both the x and y directions.

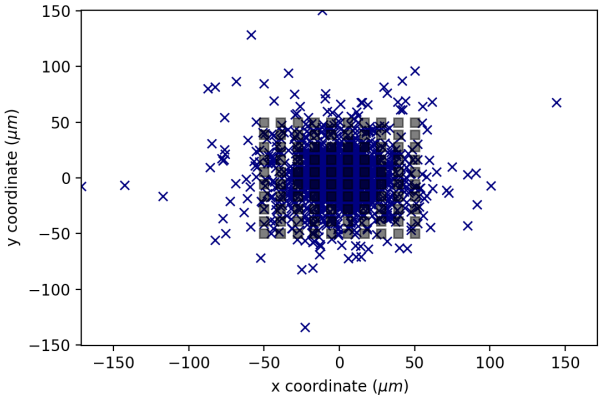

Figure 7: The blue crosses show the position of a muon, the shaded square shows the position of a nanoisland. The Gaussian beam has a standard deviation of 10μm and a mean of 0μm in both x and y directions.

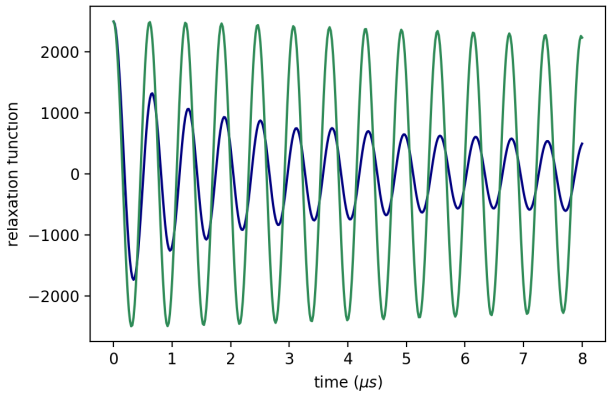

Figure 8: A plot of the relaxation function for a muon beam spot with a standard deviation of 100μm (blue line), and the relaxation function for a spot with a standard deviation of 10μm (green line). Both distributions have an r_z value of 400μm.

Seeing that we can not model the procedure of the μSR experiment shown in figure 1, where the polarisation of the muons is found using a forward and backward facing detectors, we will instead utilise the relaxation function. It has been shown that the relaxation function created from experiments can be found from the summation of the individual spin polarisations (equation 5) of each muon. Equation 8 can be fitted to the overall relaxation function to find the precession frequency, therefore the magnetic field, and relaxation rate λ of the system.

Figure 8 shows the relaxation function found from two different muon distributions, one with an x and y standard deviation of 100μm (blue line) and the other 10μm (green line) with all other variables kept constant. This change in standard deviation demonstrates the changing field distribution around the nanoislands. It is clear that λ differs a lot in the two systems, the larger standard deviation shows a greater relaxation rate. This is because the magnetic field felt by each muon is more diverse when the spread of

the muons is larger. We know that the magnetic field fall off as $1/r^3$, so the muons situated much farther from the centre of the magnet system will have phases which differ more in the system with a larger beam width than a smaller one. This leads to more damping in the oscillations of the overall relaxation function and therefore a larger λ.

Interestingly, there is also a slight shift in frequency, this implies that the two systems feel a different magnetic field even though they are the same r_z distance from the sheet. The magnetic field felt by the larger standard deviation is (118.77 ± 0.08) G whereas the magnetic field felt by the smaller standard deviation is (120.085 ± 0.001) G. The magnetic field for the larger standard deviation is slightly smaller because there are more muons being measured that are farther from the magnets. This means that when all the relaxation functions are summed the final frequency, and therefore magnetic field, will be affected.

Figure 9 shows how the relaxation function changes as the muon distribution moves farther from the magnets in the z direction. This has a larger impact on the final relaxation function of the system than changing the standard deviation. We know that the magnetic field is proportional to the frequency so it is expected that as r_z increases the frequency decreases, as is in agreement with the figure. The frequency for a mean of 1000μm is $(67.676888 \pm 0.000002)\times10^4$ Hz and for a mean of 400μm the frequency is $(1022.67 \pm 0.01)\times10^4$ Hz. Figure 10 shows how the magnetic field values are changing as r_z increases. The green line shows that the magnetic field is dropping off as $1/r^3$. The relaxation function also decreases as the muons move farther from the sheet where at a position $r_z = 400\mu$m and 10μm the relaxation function $\lambda = (1300 \pm 300)\text{s}^{-1}$ and $(3.53 \pm 0.05)\text{s}^{-1}$.

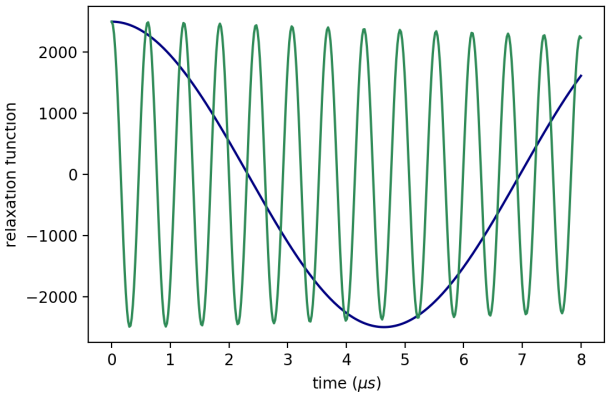

Figure 9: The relaxation function from the muons as shown in figure 7 where the muon beam spot has a Gaussian distribution with a standard deviation of 10μm, the the blue line shows the muons at an r_z position of 1000μm away from the magnetic sheet and the green line is 400μm away.

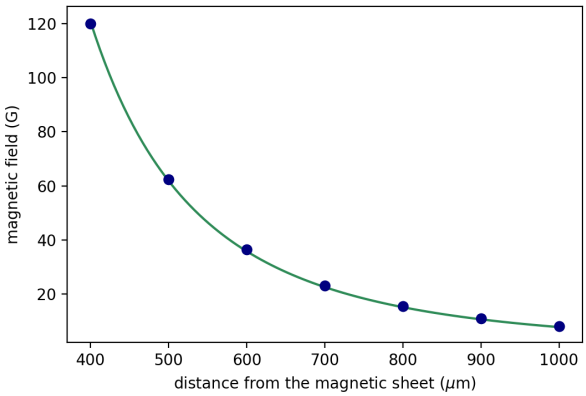

Figure 10: The magnetic field calculated from the frequency fitted to the relaxation function at different r_z distances are shown by the dots, the line is a C/r^3 fitted line where C is a scaling constant with a value of $(7.73 \pm 0.03)\times10^{-9}$.

3.4 Gaussian muon distribution in three dimensions

In experiments the muons will not be situated in a two dimensional slice, instead they are produced from a beam and implant into a stopping material. This means that there will be a distribution in the z direction. This will be modelled using another Gaussian function where the z distribution will be independent of the beam spot distribution, this model is illustrated in figures 11 and 12. Figure 11 shows the position of the individual muons for a mean of 0μm, 0μm and 100μm in the x, y and z directions

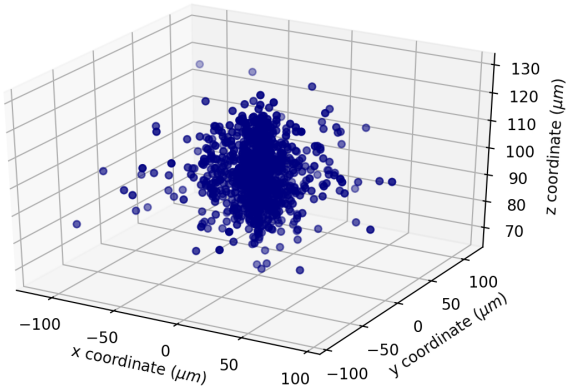

Figure 11: The position of the muons as a three dimensional beam, the magnetic sheet is positioned at $z = 0$. The mean in the x and y direction is 0μm and in the z direction it is 100μm, the standard deviation is 10μm in all three directions.

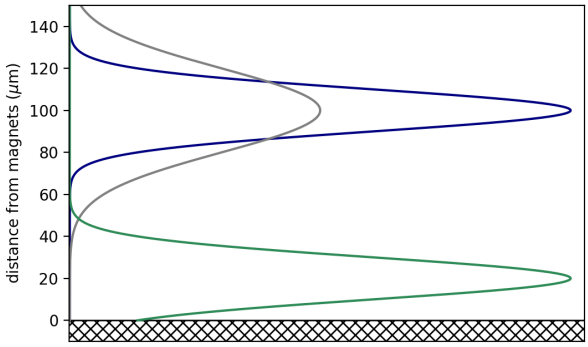

Figure 12: The lines represent the z distribution of the muons, the hatched region represents the magnetic sample. The different colours of the lines show examples of different means and standard deviations of the muons.

respectively, the standard deviation is 10μm in all three directions. Figure 12 shows the muon distribution in the z direction for different means and standard deviations. In experiments the stopping distribution is controlled by the energy of the muon beam and the thickness of the stopping material [25].

Keeping the magnetic dipoles aligned the relaxation function for each muon site can be calculated. To imitate experimental results the individual spin polarisations will be summed as before to get the overall relaxation function of the system. The relaxation function of muons positioned at different means but the same standard deviation (demonstrated by the green and blue lines in figure 12) will be compared. Figure 13 shows the relaxation distribution for muon beams with a standard deviation of 10μm in all three coordinates and with a varying r_z at 1000μm and 400μm. The relaxation rate increases by a large amount in the two systems, much larger than when the muon sites were limited to a two dimensional plane in figure 9. This implies that there is a larger difference in phase between muons in the three dimensional system than in two dimensions.

The frequency for a mean of 1000μm is $(6.7632 \pm 0.0001)\times10^5$ Hz and for a mean of 400μm the frequency is $(1.013 \pm 0.001)\times10^7$ Hz. These are very similar to the frequencies found in the two dimensional case. However, they shift slightly implying a shift in the magnetic field. As in the two dimensional case, the magnetic field as a function of distance from the magnetic sheet (the z mean of the muon distribution) is plotted and shown in figure 14. There is still a $1/r^3$ relationship even with the slight frequency shift, though it will be of interest to observe how a changing muon distribution will impact this $1/r^3$ relationship. This will be discussed in section 4.2.

Another way to see how the magnetic field distribution is changing is to compare the magnetic field felt by each muon. For an r_z mean of 1000μm and standard deviation of 10μm in all three directions a histogram of the magnetic field felt at each site is plotted in figure 15. A scaled Gaussian curve is also fitted to the data where, from this, the full width at half maximum (FWHM) can be found. The FWHM will demonstrate the spread of the magnetic field distribution in a similar way to the relaxation rate. Figure 16 shows the FWHM for different distances from the magnetic sheet. The line fitted is $1/r^6$ which is not the same drop off as the magnetic field alone but it will help us to understand what is going on with the field distribution and will show us if there is a shift from the trend found in the data.

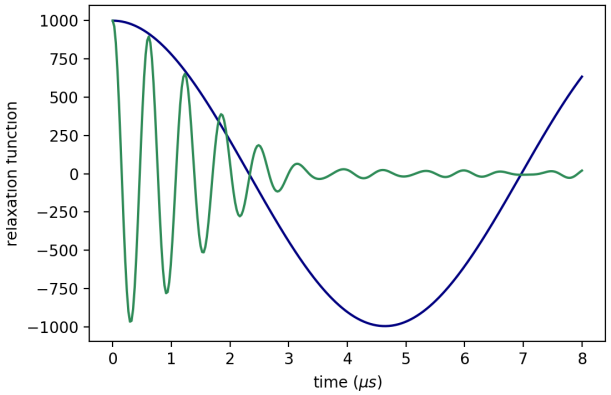

Figure 13: The relaxation function plotted for a muon distribution with a mean of 1000μm (blue line) and 400μm (green line). The standard deviation in all three coordinates is 10μm.

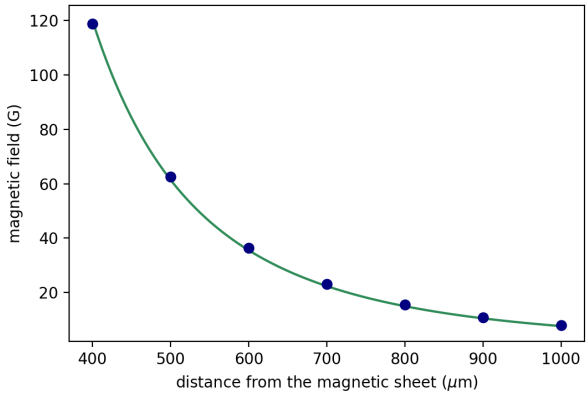

Figure 14: A C/r^3 fit to the magnetic field calculated at different r_z values of the muon distribution where the value of C was found as $(7.68 \pm 0.04)\times10^{-9}$.

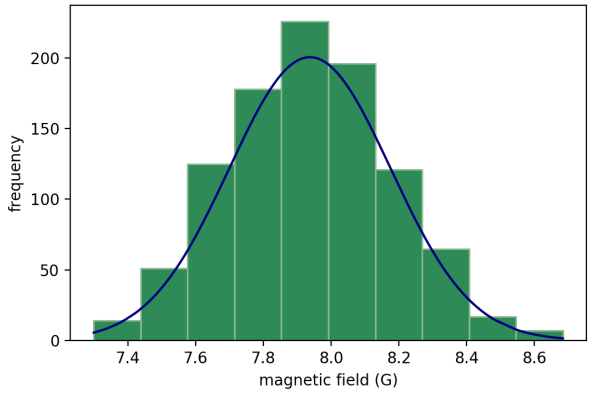

Figure 15: The relaxation function plotted for a muon distribution with a mean of 1000μm (blue line) and 400μm (green line). The standard deviation in all three coordinates is 10μm.

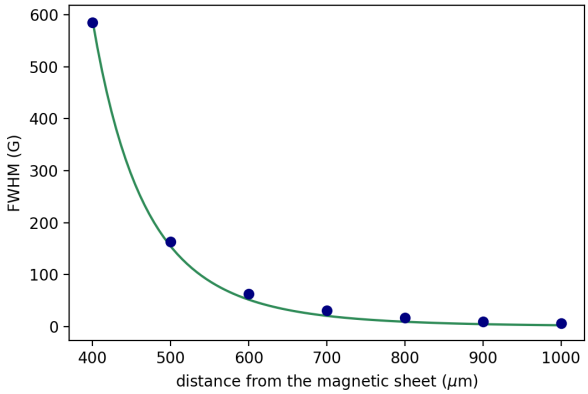

Figure 16: FWHM as a function of z coordinate r_z (dots) with a $1/r^6$ line fitted to the data.

3.5 Modelling the system

The μSR experiment was programmed in C. The input parameters are written to a configuration file (via Python code) and are read by the programme. The programme includes functions that calculate the magnetic field and create muon position grids through the methods explained above. The C code only returns the magnetic field felt by each muon site, this is then loaded into Python so that the individual muon spin polarisations can be calculated and summed. This is where the relaxation functions are found. The functions are fitted using the "curve_fit" function from the scipy module. From this the value and error of the frequency and the relaxation rate are found. The uncertainties in other parameters were found by combining them in quadrature. The majority of the error in calculation does not show up in the figures because they are relatively small, however they will be quoted when any value is stated. The

C code can be found in appendix A and the Python code in appendices B and C.

4 Discussion

4.1 Changing implantation depth distribution

The impact of the muon sites on the magnetic field measured using the aforementioned computational model can be investigated. This will enable a clearer picture of what is happening in the experiment. Let us explore the impact of changing the standard deviation of the muon implantation sites across all directions. First the standard deviation in the z direction will be changed, that is the implantation depth distribution of the muons. The mean position in x and y will be kept at 0μm, the centre of the magnetic sheet, throughout the report.

Figure 17 shows how the magnetic field is changing as a function of mean distance from the magnets, z, where the z distribution has a standard deviation of 100μm, a factor of 10 larger than in figure 14. The standard deviation in x and y is kept constant at 10μm. It is clear from the plot that there has been a shift in the magnetic field felt by the two different muon distributions. The magnetic field has both decreased in magnitude and deviated from the $1/r^3$ relationship (green line). Now the standard deviation in the z direction is larger, there are a larger number of muons farther from the magnet. Because these muons are farther from the magnet they feel a smaller magnetic field therefore the overall relaxation function will have a reduced frequency. This reduction will be larger than any increase caused by muons closer to the magnet. This is because of the $1/r^3$ drop off of the magnetic field.

With an increased standard deviation muons are distributed across a larger area decreasing their density. This means that there is a larger disparity in the magnetic field measured by each individual muon in the system. Therefore the overall magnetic field felt by the muons will not be averaged to the field at the mean position of the muons leading to a deviation from the $1/r^3$ trend. Figure 14 shows this. The shift was not as large with a smaller standard deviation of 10μm because the magnetic field felt by the system is averaged roughly to that measured at the position of the mean value r_z.

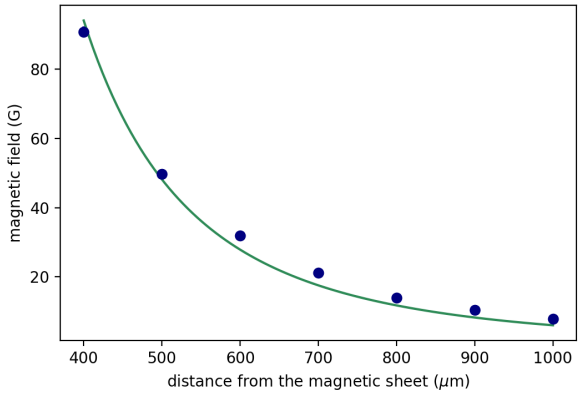

Figure 17: A C/r^3 fit to the magnetic field calculated at different mean values of the muon distribution where the value of C was found as (3.9 $\pm$ 0.2)$\times 10^{-9}$. The standard deviation in the z direction is 100μm and is 10μm in the x and y directions.

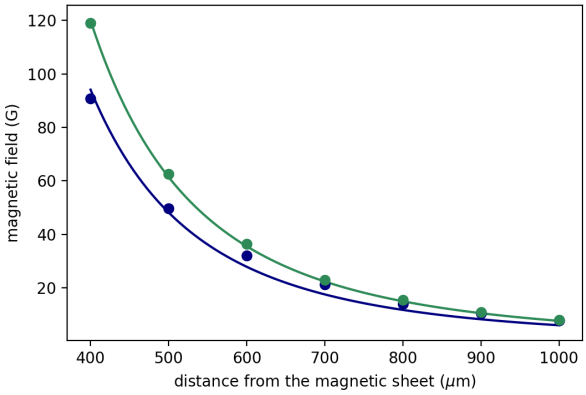

Figure 18: The plots for the magnetic field felt at different z distance for a z standard deviation of 100μm (blue line) and 10μm (green line). The x and y standard deviations are 10μm.

After a certain z distance the overall magnetic field measured from the two standard deviations tend towards each other, as shown in figure 18. This is due to the fact that as r_z gets larger the overall magnetic field will not change as much because it decays to zero.

The relaxation function for the different z standard deviations shifts to a greater extent than the magnetic fields. Figure 19 shows this. As the standard deviation gets larger there are more muons that are farther from the magnet in the z direction which affects the relaxation rate, λ. This is because the changes in the field distribution felt by the system will be much greater as the spread of muons gets larger. In the figure the standard deviations chosen were 100μm (blue line) and 10μm (green line). As there is a decrease in the standard deviation, from 100μm to 10μm, there is a decrease in power of the relaxation rate trend, from z^{-4} to z^{-5}. Again this illustrates the varying magnetic field distribution over greater volumes.

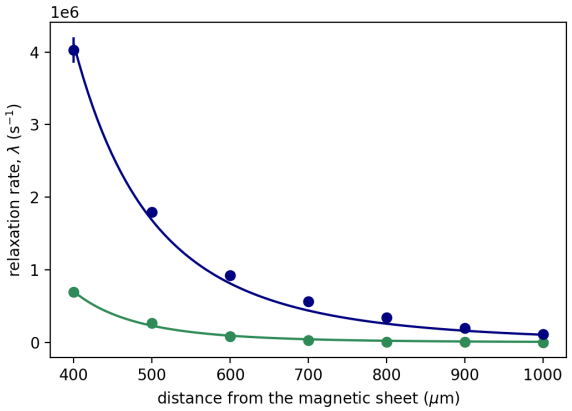

Figure 19: The relaxation rate plotted against the mean, r_z, for a standard deviation of 100μm (blue line) and 10μm (green line). The blue line shows a $1/z^4$ relationship and the green shows a $1/z^5$ relationship. The x and y standard deviations are 10μm.

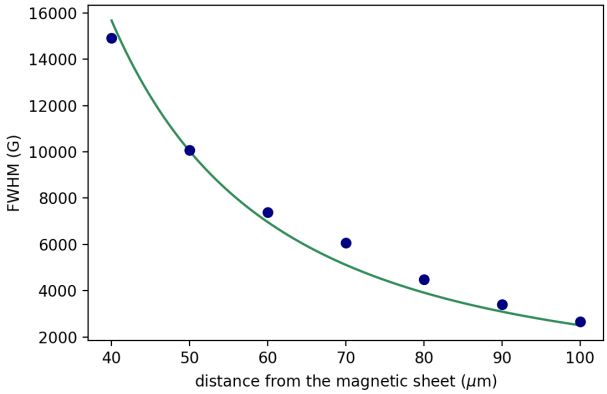

Figure 20: The FWHM plotted against the distance from the magnetic sheet, the line fitted is of the form $1/r^2$. The standard deviation is 10μm in all three coordinates.

For the overall relaxation function there comes a point where r_z decreases so much that the relaxation rate becomes very large and the frequency of the function can no longer be found. In this case the FWHM approach to analysing the magnetic field will be implemented, this is shown in figure 20. The standard deviation in all three coordinates is 10μm. It is clear that because the FWHM values increase as the distance to the magnetic sheet decreases the individual muons feel a larger variety of magnetic fields closer to the magnets. This is because the difference between the magnetic fields felt by the closest and farthest muon is much greater when r_z is small. This is, again, due to the $1/r^3$ drop off of the magnetic field. When r_z is large the difference between the value of the magnetic field of the closest and farthest muon will not be as different because the magnetic field distribution starts to become more homogeneous.

The data in figure 20 does not follow the $1/r^2$ trend between r_z mean values of 60 to 90μm which is interesting. This implies that at certain distances the field distribution detected is not changing consistently as a function of r_z. This could be due to the number of muons in the system, so far all the figures have shown a system with 1000 muons. If it is because of the number of muons then if this is increased it should show a more consistent trend. The data is compared to that of a system with 15625 muons in figure 21. As is clear in the figure, when the muon is 40μm away from the magnetic sheet the FWHM is much larger for

the system with a large number of muons. This is because the density of muons has increased and the number of muons feeling larger magnetic fields will also have increased. This is because there is a greater probability of a muon being positioned closer to the magnetic sheet due to the nature of the Gaussian profile. From this the field distribution measured by the system will be changing dramatically leading to a large FWHM and implying a large relaxation rate. A limitation of this model is that the muons may be positioned between the dipoles leading to a large FWHM. This becomes more likely as the number of muons increases. In a μSR experiment this would not happen.

When r_z becomes farther from the sheet then the different systems starts to have similar FWHM values as seen by the inset in the figure. The fact that the data points start to agree means that the number of muons is not the factor that is causing the system to deviate from the apparent trend of the FWHM. Instead it may have to do with the Gaussian distribution of the muons.

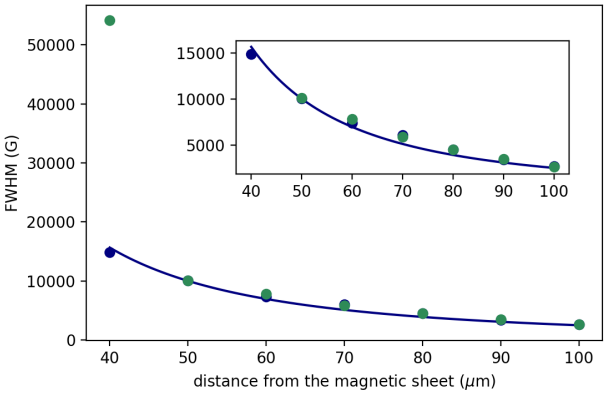

Figure 21: The FWHM rate plotted against the r_z for a z standard deviation of 100μm where the number of muons in the stopping material is 1000 (blue dots) and 15625 (green dots). The line is a $1/r^2$ fit to the data with 1000 muons. The x and y standard deviations are 10μm.

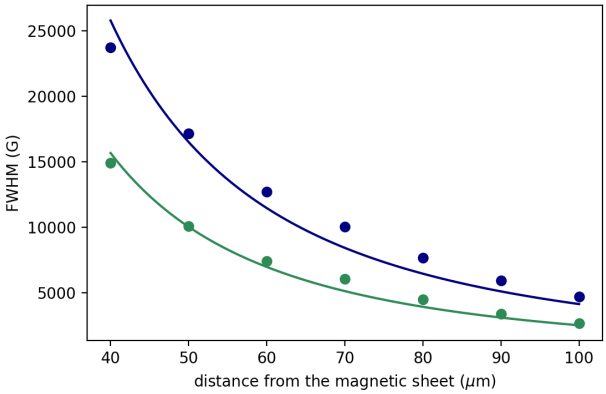

Figure 22: The FWHM rate plotted against r_z for an x and y standard deviation of 100μm (blue line) and 10μm (green line). They both have a fitted $1/r^2$ line to compare the two sets of data. The z standard deviation is 10μm.

Returning the number of muons to 1000 the trend of the FWHM can be seen to change when the x and y standard deviations are different, shown in figure 22. The standard deviations chosen were 100μm (blue line) and 10μm (green line). The overall FWHM at each r_z value reduces as the standard deviation reduces shown by the lines of the two systems differing. Since a larger standard deviation causes there to be more muons farther from the magnetic sheet there is a larger variety of magnetic field values felt. This describes a less uniform magnetic field distribution. This is consistent with the plot and agrees with the explanation given for figure 19. The overall drop off of the FWHM is not the same for the two systems as demonstrated by fitting a $1/r^2$ line to both of the data sets. For the larger standard deviation the trend has become more linear. This is because the density of muons is smaller. If the density is smaller, then the magnetic field distribution felt by the system will not vary as much when the muon distribution is moved farther from the magnets. There may be a standard deviation large enough that the FWHM does not change as a function of r_z.

The magnetic moments of the nanoislands may not always be aligned, they could be randomised. Figure 23 shows the relaxation function for a magnetic sheet with randomly generated magnetic moment

directions. Comparing this to figure 13 it can be seen that the frequency has increased for both of r_z values. This means that the magnetic field overall has increased. It is also interesting to see that the relaxation rate is not the same. The relaxation function decays to a non-zero value as consistent with the Kubo-Toyabe function shown in figure 2. When the z standard deviation is increased the relaxation rate increases again, as it does when the magnetic moments aligned, where figure 24 behaves more like a typical Kubo-Toyabe function.

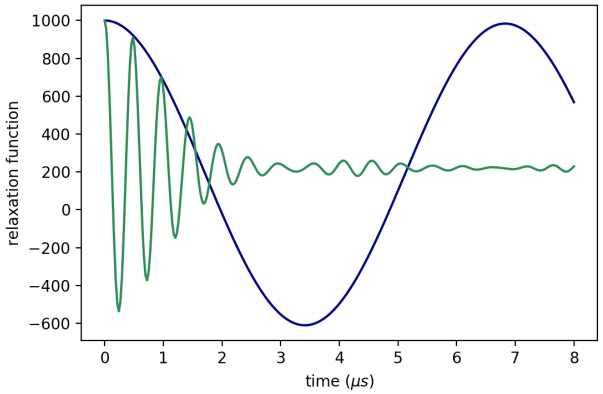

Figure 23: The relaxation function for a muon distribution with a standard deviation of 10μm in all three coordinates and with a mean of 1000μm (blue line) and 400μm (green line).

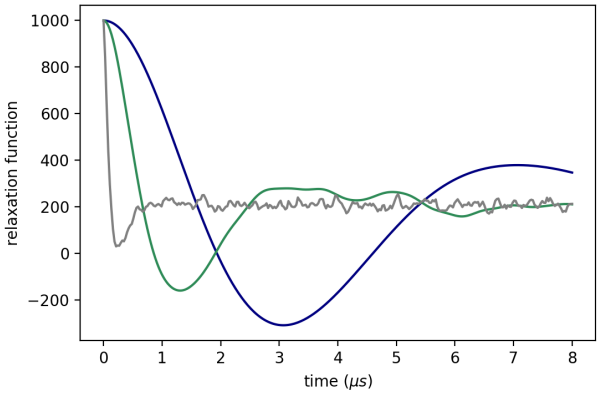

Figure 24: The relaxation function plotted for muon distributions with an x and y standard deviation of 10μm and a z standard deviation of 100μm. The blue line has a z mean of 1000μm, the green has a mean of 700μm and the grey line has a mean of 400μm.

Figures 25 and 26 show how the different standard deviations in the x and y directions shift the overall magnetic field and relaxation rate, respectively. In the magnetic field plot the muon distribution with an x and y standard deviation of 100μm (blue line) has a $1/r^3$ line fitted to it. From 500 to 600μm the magnetic field values deviate from the $1/r^3$ trend as it does in the case of aligned magnetic moments (figure 17). Although, unlike the case with aligned magnetic moments, the magnetic field seems to return to the $1/r^3$ trend. The deviation may may be due to the random field distribution. This also happens with the relaxation rate. In the case with the smaller standard deviation of 10μm neither the magnetic field nor the relaxation rate deviate from their respective trends. This is because, as with the aligned magnetic moments, the standard deviation is small so the variety of different magnetic fields felt by each muon in the system will not be as large as with a bigger standard deviation.

With the relaxation rate in figure 26 the lines that are fitted to both data sets are the same functions as that for the aligned magnetic moments. As the standard deviation reduces from 100μm to 10μm the trend the respective data sets follow reduce from a $1/r^4$ trend to a $1/r^5$ trend due to the more diverse magnetic field distribution felt by the muons implanted with a larger standard deviation. This again illustrates how the magnetic field distribution is changing as the muon distribution changes. It is interesting that the alignment of the magnetic moments does not affect how the overall trends of the data behave. The values of the magnetic field and relaxation rate, however, do change. The magnetic field felt by the muons with randomised magnetic moments differs by approximately 20G when comparing figures 18 and 25. The relaxation rate shifts from: for random magnetic moments $(5.8 \pm 0.2)\times10^6\ s^{-1}$ to aligned magnetic moments $(3.4 \pm 0.1)\times10^6\ s^{-1}$ for the mean position of z at 400μm. The reason the relaxation rate is

larger for randomised magnetic moments is because the field distribution cause by a randomly generated magnetic sheet will not be as uniform as that for an aligned magnetic sheet. After a certain r_z value both magnetic sheets would have similar magnetic field distributions because the field lines from the randomly generated sheet will have smoothed out. As r_z gets closer to the magnetic sheet the field distribution will be varying a lot more leading to a large relaxation rate.

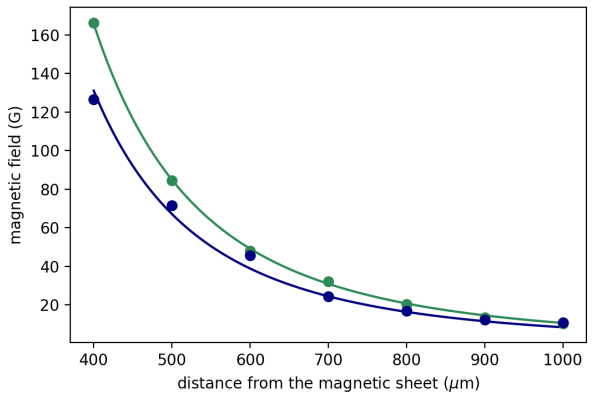

Figure 25: The relaxation function plotted for a muon distribution with an x and y standard deviation of 100μm (blue line) and 10μm (green line). The standard deviation in the z coordinates is 10μm. Both data sets are fitted with a $1/r^3$ line and the magnetic moments are now randomised.

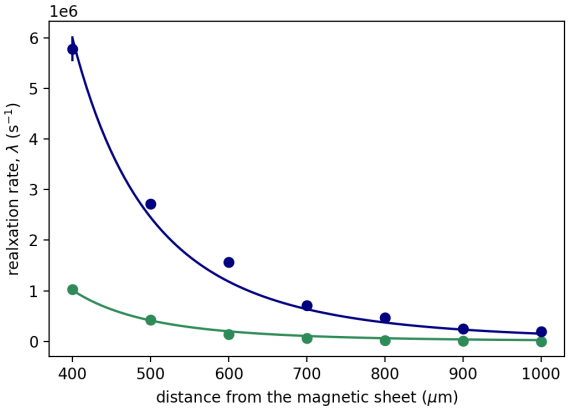

Figure 26: The relaxation function plotted for a muon distribution with an x and y mean of 100μm (blue line) and 10μm (green line). The standard deviation in all three coordinates is 10μm. The blue line is a fitted $1/r^4$ line and the green line is $1/r^5$. The magnetic moments are now randomised.

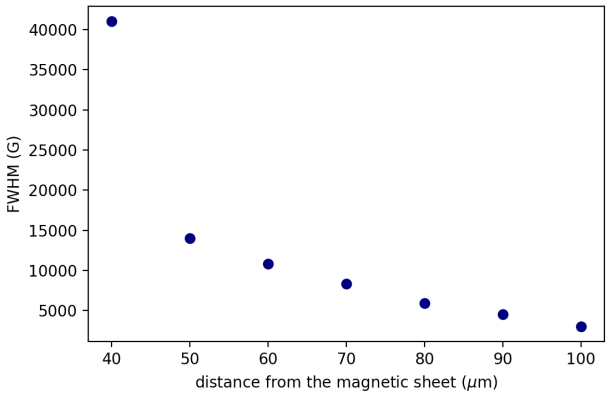

Figure 27: The FWHM plotted for a muon distribution with a standard deviation of 10μm in all three coordinates.

When the function decays too quickly the relaxation rate and the frequency of the relaxation functions can not be measured when the muon distribution gets very close to the magnetic sheet. So, the FWHM for a muon distribution with a standard deviation of 10μm in all three coordinates and a varying z mean

will be looked at. If the point at a z mean of 40μm is ignored then the FWHM decreases almost linearly as the distance away from the magnetic sheet increases. The reason that the point at a mean of 40μm is so different to the rest of the other points is that as the muon distribution gets closer to the magnetic sheet there is a higher probability that there will be muons extremely close to large magnetic field values. This tells us that the field distribution is not as uniform closer to the sheet.

4.2 Changing beam spot size

As well as being able to control the implantation depth, the muon beam size can also be adjusted. To see the affects of the beam size changing, the standard deviation in the x and y directions will be changing. Figure 28 shows how the relaxation function changes with a changing standard deviation. The change is small between the three lines, but there is a change in the measured magnetic field and relaxation function. There are equal step sizes between the standard deviations of each relaxation function, from figure 28 alone it can be seen that the relaxation rate and frequency of each function is changing non-linearly. Figure 29 illustrates this more clearly. This is a plot of the relaxation rate as a function of standard deviation. A line of the form $a\exp(b\sigma)+c$ is fitted to the data to demonstrate how the relaxation rate increases at an increasing rate. This is because as the standard deviation gets bigger, a larger number of muons are feeling a smaller magnetic field. This change is not as drastic as when r_z is changing because there are still a number of muons that are measuring the field at the centre of the distribution. The relaxation rate changing so much demonstrates how the field distribution is varying as the muon distribution is moving spatially.

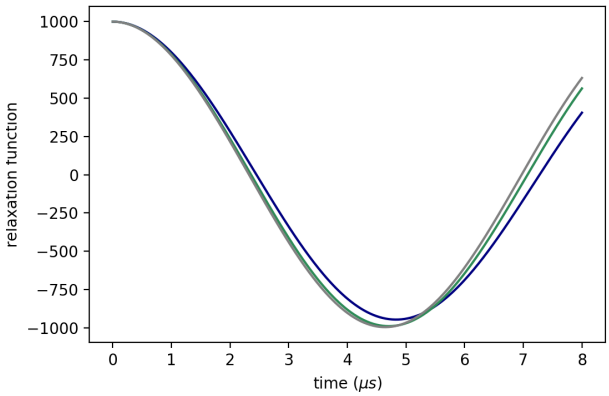

Figure 28: The relaxation function plotted as a function of time. The blue line shows the largest x and y standard deviation at 100μm, and the grey line with the smallest standard deviation at 10μm where the green line has a standard deviation between the two.

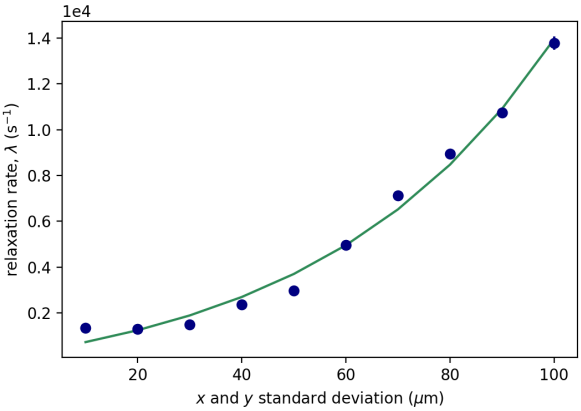

Figure 29: The relaxation function plotted as a function of x and y standard deviation. The fitted curve is an exponential of the form $a\exp(b\sigma)+c$ where σ is the standard deviation value in x and y. a, b and c were found to be (1700 ± 700), $(22\,000\pm3000)\text{m}^{-1}$ and (-1400 ± 900), respectively.

The magnetic field, however, behaves in a different way as a function of standard deviation. The slight frequency shift in figure 28 already indicates a varying magnetic field. Figure 30 shows how the magnetic field decreases linearly as the muon beam becomes more spread out. From 0μm to roughly 20μm the magnetic field keeps a similar value, when the beam spot is small enough the magnetic field will not vary much. This is due to the magnetic field distribution varying by smaller amounts as the volume that is being examined decreases. This is also represented by the relaxation rate in figure 29 almost becoming

constant as it tends towards smaller standard deviations.

Figure 31 shows the relaxation rate of muons with an r_z of 100μm and varying x and y standard deviations. It is shown that as the standard deviation increases the relaxation rate also increases, as one would expect. This has already been explained in section 4.1.

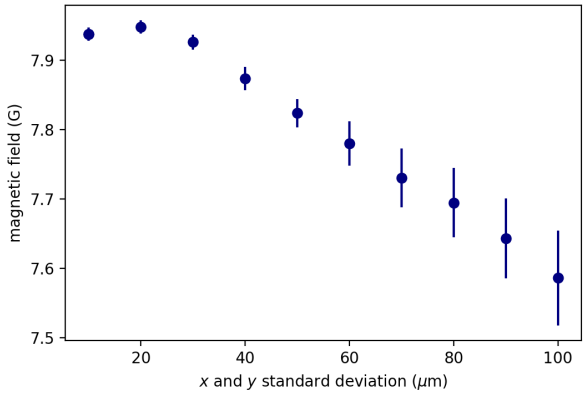

Figure 30: For a changing x and y standard deviation and a z mean of 1000μm the magnetic field calculated is plotted where the z standard deviation is kept at 10μm.

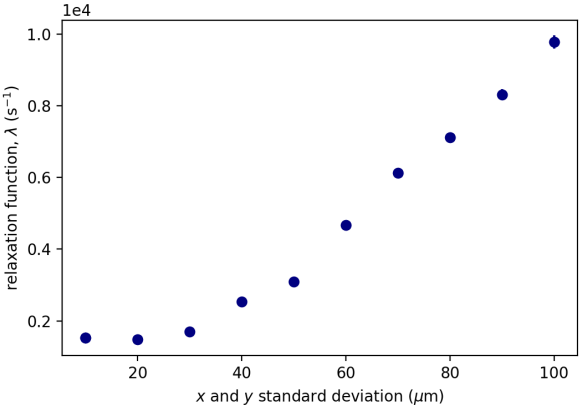

Figure 31: The FWHM rate plotted against the x and y standard deviations for a mean z position of 100μm.

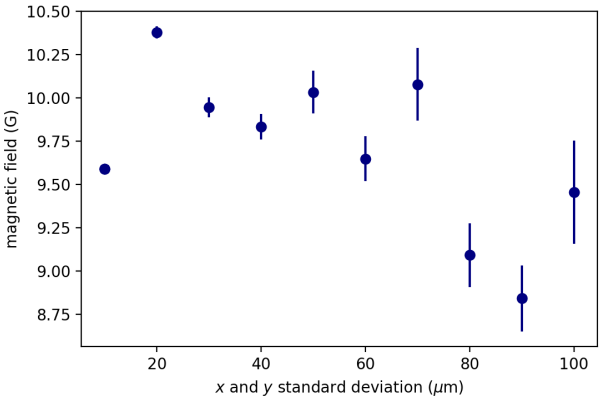

Figure 32: For a changing x and y standard deviation and a z mean of 1000μm the magnetic field calculated is plotted where the z standard deviation is kept at 10μm for randomly orientated magnets.

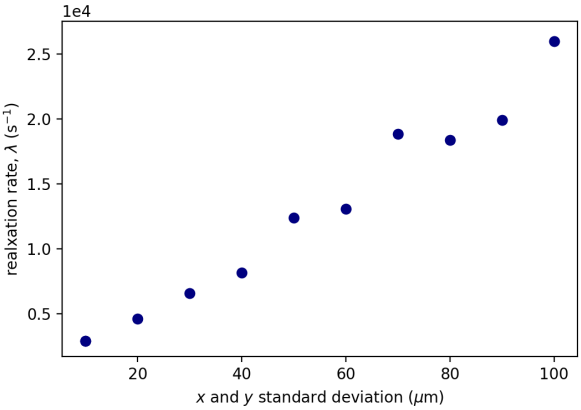

Figure 33: The relaxation rate plotted against the x and y standard deviations for a mean z position of 100μm for randomly orientated magnets.

For randomly orientated magnets the same variables were chosen and plotted in figures 32 and 33. Looking at how the magnetic field changes as a function of standard deviation in figure 32 it seems surprising that there is no noticeable correlation between the points. This is due to the random nature of the magnetic sheet. As the standard deviation gets bigger there is a larger variety of magnetic fields felt by each

muon. At each standard deviation a new magnetic sheet is generated and therefore a new magnetic field distribution. This leads to differing magnetic fields felt by the different systems. The magnetic fields felt, however, are very similar where they are only varying by approximately 2 G telling us that the magnetic field at each standard deviation is approximately the same.

In figure 33 it is shown that there is a linear relationship between the spot size of the beam and the relaxation rate of the muon. This follows the same relationship as with the magnetic sheet full of aligned magnets, the only difference is that for the aligned magnets the relaxation rate starts to become a constant value at small standard deviations. This is not what is seen with randomly orientated magnets. This is because the field distribution will still be relatively varied close to the magnetic sheet due to the random magnetic moments.

5 Conclusion

The muon distribution in the μSR experiment may return predictions of magnetic field distributions that may not follow some trends that are expected. These show themselves in shift of frequencies and relaxation rates.

It has been shown that there is a shift in magnetic field as the implantation depth of the muon beam is changed. Usually there is a $1/r^3$ drop off of a magnetic field but this correlation seems to not hold as some of the parameters of the muon distribution are changed. Specifically as the z standard deviation of the distribution increases this is when the magnetic field starts to deviate from this $1/r^3$ relationship. This is due to the density of muons decreasing, meaning the magnetic distribution felt is more uniform. As the beam spot size increases the magnetic field starts to drop off linearly after a certain value of beam spot standard deviation. Albeit the change is small, but this shift in magnetic field is an interesting occurrence and is due to the fact that more muons are situated farther from the magnetic film. When random magnetic moments are implemented instead of aligned ones there is also a shift in frequency. The frequency, and therefore magnetic field increases when the only variable that changes is the direction of the magnetic moments. This has something to do with the random nature of the magnetic field distribution.

In regard to the relaxation rate, this drops off as a function of implantation depth as would be expected. What is interesting is as the beam spot size gets smaller, the relaxation rate drop off starts to decrease. This is due to the changing field distribution, for a small standard deviation the field distribution will not be varying as much because it is confined to a smaller volume. This means that there is a smaller variation in relaxation function, leading to a different decrease in relaxation rate as a function of standard deviation. For aligned magnetic moments the magnetic field drops off is linear and the relaxation rate increases linearly as a function of standard deviation. This tells us that the muons feel a less homogeneous magnetic field distribution as the beam size gets larger. For randomly oriented magnetic moments the magnetic field measured has no correlation, it changes with each standard deviation step. This is because the field distribution is not the same as in the aligned case. The random field distribution allows this varying magnetic field. The relaxation rate, however, increases linearly as in the aligned magnetic moment case.

Overall the shape and size of the muon distribution in μSR experiments varied the output relaxation function. The experiment has been modelled such that different parameters can be changed in order to more deeply understand how muons behave within the stopping material. This can be compared alongside experimental data to see if stopping muons outside of a sample creates a system that detects magnetic dipole contributions uniformly.

There are various modifications that can be made to the model such as simulating the muon implantation profile using models such as TRIM.SP. The single dipole approximation to the nanoisland structure can

be modified so that there is a multiple dipole approximation. Also, the model should set boundaries to the muon distribution so that there are no muons implanted inside the magnetic sheet.

References

[1] S. H. Neddermeyer and C. D. Anderson, "Note on the nature of cosmic-ray particles," *Phys. Rev.*, vol. 51, pp. 884–886, May 1937.

[2] E. Y. Vedmedenko, H. P. Oepen, and J. Kirschner, "Size-dependent spin reorientation transition in nanoplatelets," *Physical Review B*, vol. 67, January 2003.

[3] B. E. Kane, "A silicon-based nuclear spin quantum computer," *Nature*, vol. 393, pp. 133–137, May 1998.

[4] E. Morenzoni, F. Kottmann, D. Maden, B. Matthias, M. Meyberg, T. Prokscha, T. Wutzke, and U. Zimmermann, "Generation of very slow polarized positive muons," *Physical Review Letters*, vol. 72, no. 17, pp. 2793–2796, 1994.

[5] E. Morenzoni, H. GlÃijckler, T. Prokscha, H. P. Weber, E. M. Forgan, T. J. Jackson, H. Luetkens, C. Niedermayer, M. Pleines, M. Birke, A. Hofer, J. Litterst, T. Riseman, and G. Schatz, "Low-energy musr at psi: present and future," *Physica B: Condensed Matter*, vol. 289-290, pp. 653–657, Aug. 2000.

[6] S. R. Giblin, J. D. M. Champion, H. D. Zhou, C. R. Wiebe, J. S. Gardner, I. Terry, S. Calder, T. Fennell, and S. T. Bramwell, "Static magnetic order in tb2sn2o7 revealed by muon spin relaxation with exterior muon implantation," *Physical Review Letters*, vol. 101, p. 237201, Dec. 2008.

[7] A. Berlie, I. Terry, S. Giblin, T. Lancaster, and M. Szablewski, "A muon spin relaxation study of the metal-organic magnet Ni(TCNQ)2," *Journal of Applied Physics*, vol. 113, p. 17E304, Apr. 2013.

[8] R. F. Kiefl, M. D. Hossain, B. M. Wojek, S. R. Dunsiger, G. D. Morris, T. Prokscha, Z. Salman, J. Baglo, D. A. Bonn, R. Liang, W. N. Hardy, A. Suter, and E. Morenzoni, "Direct measurement of the london penetration depth in yba2cu3o6 using low-energy musr," *Physical Review. B, Condensed Matter and Materials Physics*, vol. 81, no. 18, p. 180502, 2010.

[9] W. Eckstein, *Computer Simulation of Ion-Solid Interactions*. Springer Series in Materials Science, Berlin Heidelberg: Springer-Verlag, 1991.

[10] C. Niedermayer, "Muon spin rotation studies of doping in high-t c superconductors," *Acta Physica Polonica A*, vol. 96, no. 2, pp. 213–227, 1999.

[11] T. Jackson, C. Binns, E. Forgan, E. Morenzoni, C. Niedermayer, H. Gluckler, A. Hofer, H. Luetkens, T. Prokscha, T. Riseman, A. Schatz, M. Birke, J. Litterst, G. Schatz, and H. Weber, "Superparamagnetic relaxation in iron nanoclusters measured by low energy muon spin rotation," *Journal Of Physics-Condensed Matter*, vol. 12, pp. 1399–1411, February 2000.

[12] S. Calder, S. R. Giblin, and S. T. Bramwell, "Using ÎijSR as a magnetometer," *Physica B: Condensed Matter*, vol. 404, pp. 1017–1019, Apr. 2009.

[13] R. C. Johnson, B. Z. Malkin, J. S. Lord, S. R. Giblin, A. Amato, C. Baines, A. Lascialfari, B. Barbara, and M. J. Graf, "Evolution of spin relaxation processes in liy(1-x)hoxf4 with increasing x studied via ac-susceptibility and muon spin relaxation," July 2012.

[14] A. Hillier, P. King, S. Cottrell, and J. Lord, "The musr user guide," *ISIS Facility, STFC, Rutherford Appleton Laboratory, UK*, 2005.

[15] Z. Salman, S. J. Blundell, S. R. Giblin, M. Mannini, L. Margheriti, E. Morenzoni, T. Prokscha, A. Suter, A. Cornia, and R. Sessoli, "Proximal magnetometry of monolayers of single molecule magnets on gold using polarized muons," *arXiv:0909.4634 [cond-mat]*, Sept. 2009. arXiv: 0909.4634.

[16] S. L. Lee, S. H. Kilcoyne, and R. Cywinski, *Muon science: Muons in physics, chemistry and materials*. IOP Publishing, 1999.

[17] R. H. Heffner and D. G. Fleming, "Muon spin relaxation," *Physics Today*, vol. 38, pp. 65–112, 1984.

[18] S. Blundell, *Magnetism in Condensed Matter*. Oxford Master Series in Condensed Matter Physics, OUP Oxford, 2001.

[19] S. J. Blundell, "Spin-polarized muons in condensed matter physics," *Contemporary Physics*, vol. 40, pp. 175–192, Mar. 1999.

[20] R. Kubo and T. Toyabe, "Magnetic resonance and relaxation," 1967.

[21] I. McKenzie, "The positive muon and musr spectroscopy: powerful tools for investigating the structure and dynamics of free radicals and spin probes in complex systems," *Annu. Rep. Prog. Chem., Sect. C: Phys. Chem.*, vol. 109, pp. 65–112, 2013.

[22] T. H. Boyer, "The force on a magnetic dipole," *American Journal of Physics*, vol. 56, pp. 688–692, Aug. 1988.

[23] R. J. Holmberg and M. Murugesu, "Adhering magnetic molecules to surfaces," *Journal of Materials Chemistry C*, vol. 3, pp. 11986–11998, nov 2015.

[24] G. E. P. Box and M. E. Muller, "A Note on the Generation of Random Normal Deviates," *The Annals of Mathematical Statistics*, vol. 29, pp. 610–611, June 1958.

[25] E. Morenzoni, H. GlÃijckler, T. Prokscha, R. Khasanov, H. Luetkens, M. Birke, E. M. Forgan, C. Niedermayer, and M. Pleines, "Implantation studies of keV positive muons in thin metallic layers," *Nuclear Instruments and Methods in Physics Research Section B: Beam Interactions with Materials and Atoms*, vol. 192, pp. 254–266, May 2002.